EVALUATION OF RESOLVING POWER AND MTF OF DMC

E. Honkavaara[1], J. Jaakkola[1], L. Markelin[1], S. Becker[2]

[1]Finnish Geodetic Institute, Masala, Finland – (eija.honkavaara, juha.jaakkola, lauri.markelin)@fgi.fi
[2]University of Stuttgart, Institute for Photogrammetry, Stuttgart, Germany – susanne.becker@ifp.uni-stuttgart.de

Commission I, WG I/4

KEY WORDS: Aerial Digital Camera, Calibration field, CCD, Photogrammetry, Quality, Resolution

ABSTRACT:

The present article reports the results of an extensive empirical evaluation of spatial resolution of a digital large format Intergraph DMC sensor. The parameters of the study were flight direction, ground sample distance (GSD) and the distance from the image center. The key finding of the study was that the resolution of the DMC panchromatic large-format image was clearly dependent on the distance from the image center. One reason for this behavior is that the DMC large-format image is composed of four oblique images; the resolution of the oblique images is reduced towards the image border due to the scale reduction and projective distortion. From the image pixel size of 12 μm of DMC, a nominal resolving power value (RP) 84 lines/mm can be derived. Maximal resolution reduction factors in the image corners, caused by the image tilt, were 1.6 in the cross-flight direction and 1.4 in the flight direction. The distance from the image center did not appear to affect the resolution of the low-resolution multi-spectral images looking towards nadir. The observed MTFs indicated attractive behavior. The AWAR values of the panchromatic images were between 61 and 71 lines/mm, which is 1.2-1.4 times the nominal RP-value. Other important findings were the effects of GSD and flight direction on the resolution; these properties evidently characterize the behavior of the entire photogrammetric system tested. The image restoration by a linear restoring finite impulse response filter provided a constant resolution improvement factor of 1.4.

1. INTRODUCTION

A key quality component of the photogrammetric sensors is spatial resolution. In the case of digital sensors, the pixel size limits the spatial resolution attainable. However, in practice the nominal resolution is seldom achieved due to blur and noise caused by many factors. Key factors affecting the image resolution are the camera (e.g. optic, CCD, forward motion compensation), the system (e.g. mount, camera port glass), the flight factors (e.g. flight altitude, flight velocity, aperture, exposure), atmosphere and object factors (e.g. sun height, air turbulence, visibility) and data post processing (Hakkarainen, 1986; Read & Graham, 2002). Due to the large number of factors involved, it is crucial to test the performance of the entire photogrammetric production line empirically.

In the case of the DMC, fundamental factors affecting sensor resolution are the properties of the CCD, the optics, the TDI forward motion compensation, the resampling process where the large-format panchromatic images are generated from oblique medium-format images, and the pansharpening process of the multi-spectral images. (Hinz et al., 2000; Tang et al., 2000)

The objective of this study is to investigate the resolution of the Intergraph DMC digital large-format photogrammetric sensor. The results are of importance for the further development of test field based calibration methods, for the understanding of the performance of the digital sensors, for the selection of appropriate GSDs for practical mapping tasks, and for evaluating the performance of the photogrammetric system. The test set up is described in Section 2. The results are given in Section 3 and the most important findings are summarized in Section 4.

2. EXPERIMENTAL STUDY

2.1 DMC test flights

DMC test flights were performed at the permanent Sjökulla test field of the Finnish Geodetic Institute (FGI) (Kuittinen et al., 1994; Kuittinen et al., 1996; Ahokas et al., 2000; Honkavaara et al., 2006) on September 1-2, 2005. The test flights were performed in co-operation with the National Land Survey of Finland (NLS). The survey aircraft was the OH-ACN belonging to the NLS (Rockwell Turbo Commander 690A turbo twin-propeller aircraft with a pressurized cabin and two camera holes). The weather conditions during the campaign were excellent. The DMC was mounted on a T-AS gyro-stabilized suspension mount. Images with 5 cm and 8 cm ground sample distance (GSD) were studied (d1_g5, d1_g8a, d1_g8b; Table 1). Two similar blocks with 8 cm GSD were collected in consecutive days. Resolution targets were located in different parts of the image (Figure 1). The raw images collected were processed using DMC Post processing software (Version 4.5). Only linear tonal transformations were applied in the image processing; 16 bit/pixel images were used.

Analog reference images were collected simultaneously by a RC20 belonging to the NLS (the exposures were not synchronized). Panchromatic and color films, and a 150 mm wide-angle optic were used. The camera mount was a PAV 11A-E (not gyro-stabilized) and FMC was applied. The films were scanned by a Leica Geosystems DSW 600 scanner with a 15 μm pixel size and 8 bit/pixel pixel depth.

2.2 Methods

A permanent dense bar target and a portable Siemens star were used to evaluate the spatial resolution. The dense bar target is a 4-bar square-wave target (Figure 2) made of gravel. The target is aligned in two perpendicular directions. The widths of the

Table 1. Test blocks (n/a=not available due to missing metadata)

Block	d1_g5	d1_g8a	d1_g8b
Date	1.9.2005	1.9.2005	2.9.2005
Time	10:25-11:14	11:24-11:53	9:56-10:09
GSD (cm)	5	8	8
Optic (mm)	120	120	120
Flying speed (m/s)	77	87	n/a
Exposure (ms)	6.3*	6.0*	n/a
f-stop	11	11	n/a
Flying height (m)	500	800	800
Scale	1:4167	1:6667	1: 6667
Swath width (m)	691	1106	1106
Overlaps (%)	p=q=60	p=80, q=60	p=80, q=60

*) Automatic exposure, average

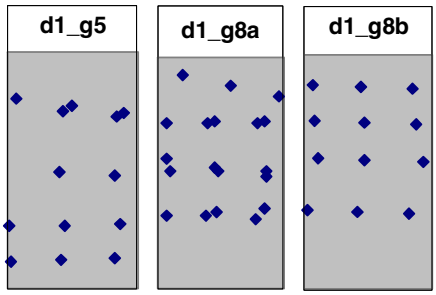

Figure 1. Distribution of resolution targets on images.

bars varies from 3 cm to 12 cm, and the bar width increment is $\sqrt[6]{2}$ (≈12%). In this study, the low contrast target (contrast 1:2) was used. The portable Siemens star (a semicircle) has 10º sectors and a 6.8 m radius; the maximum sector width is 1 m (Figure 3). Contrast is 1:5-1:11, depending on the wavelength.

The resolution evaluation was based on the resolving power (RP) and the modulation transfer function (MTF). The resolution was measured in the flight and in the cross-flight directions. In order not to reduce the quality of the analysis by subjective interpretation, highly automated methods have been implemented in the FGI's own RESOL software for the measurement of bar targets and Siemens star. RESOL version 3.0.4 was used in the study.

2.2.1 Measurement of bar targets. In the first RESOL version, the RP was calculated from microdensitometer profiles (Kuittinen et al., 1996; Ahokas et al., 2000) but nowadays 8 or 16 bit/pixel digital images are used. Several types of bar targets with different combinations of line width, space and number can be measured.

After loading the image, the position of the center profile of the test target is marked. Because the target is typically slightly rotated, the intensity values of the profile points are calculated using bilinear interpolation. The required number of parallel profiles is then generated at a distance of one pixel from the neighboring profile. The program locates iteratively the maximum and minimum points on each profile using also geometric constraints set by the dimensions of the target on the ground. A certain frequency on a profile is accepted as recognized if:

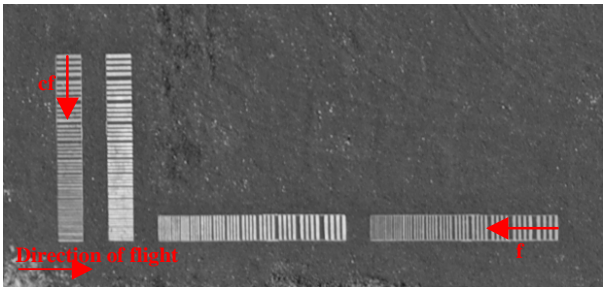

Figure 2. Dense resolution bar target. Direction of resolution measurement: cf: cross-flight, f: flight.

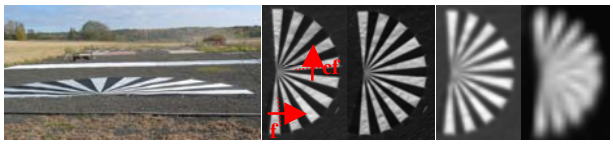

Figure 3. Portable Siemens star on ground and with 4 cm, 8 cm, 25 cm and 50 cm GSD. Direction of resolution evaluation cf: cross flight, f: flight; flying direction is from left to right or right to left.

1. All minimum and maximum points of the frequency are found to be in correct geometry, and
2. The difference between means of maximum and minimum values exceeds the combined standard deviation of maximum and minimum values multiplied by a parameter value. The parameter can be defined empirically by comparing results with visually defined values. A commonly used value is 2.

A frequency is regarded as recognized if it is accepted on more than 50% of all profiles. Finally, the MTF curves are calculated from the same profiles using equations 1-3, if necessary.

The RP, true ground sample distance (TGSD; width of the smallest detectable line on ground), and area weighted average resolution (AWAR; Ahokas et al. 2000) are calculated on the basis of the highest recognized frequency.

2.2.2 MTF determination from Siemens star. The method in the RESOL software is based on the Stuttgart method described by Becker et al. (2005, 2006). First of all, the contrast transfer function (CTF) is obtained as the quotient of the image and the object modulations (M):

$$M = \frac{I_{\max} - I_{\min}}{I_{\max} + I_{\min}} \quad (1)$$

$$CTF = \frac{M_{image}}{M_{object}} \quad (2)$$

The object modulation is obtained from the image using minimum and maximum values from a sufficiently large area of the background and object materials. As the targets are square wave targets, the CTF is transformed to MTF by series conversion (Coltman 1954). Typically the observed MTF is evaluated. For the further analyses a Gaussian shape function is fitted to the obtained MTF data (Becker et al., 2005; 2006):

$$MTF \cong e^{-2\pi^2 \sigma_{MTF}^2 K^2}, \quad (3)$$

where K is the frequency in cycles/pixel.

After measuring an approximate center point of the Siemens star, the RESOL software performs the following steps to determine the MTF:

1. Defines the radius of the star and creates circular intensity profiles.
2. Locates the edge points between white and black sectors.
3. Calculates straight lines for edges and the center point as the intersection of these lines.
4. Collects intensity data from bisections of the sectors.
5. Calculates MTF from selected sectors (vertical and horizontal sector pairs or quarter circle).
6. Fits the Gaussian shape function to the observed MTF. Parameters are σ_{PSF} (or σ_{MTF}) and an additional scaling factor to compensate for the missing 0-frequency value.

In this study, the MTF was calculated for sector pairs in flight and cross-flight directions, and for all directions using a quarter of the Siemens star (the sector pairs aligned in the flight direction, perpendicular to flight direction, and between these). From the MTF, various measures of resolution can be derived. In this study, the standard deviation of the Gaussian shape point-spread function (σ_{PSF}; Becker et al., 2005; 2006) and 10% MTF (an estimate of the RP-value) were used.

2.2.3 Image restoration. Resolution evaluation and restoration of the high-resolution panchromatic images was performed at the Institute of Photogrammetry at Stuttgart. The methods are described in detail by Becker et al. (2005, 2006).

3. RESULTS

3.1 Theoretical expectations

The large-format panchromatic image of size 7680 x 13824 pixels (92.16 mm x 165.888 mm) is composed of four medium-format images of size 4096 x 7168 pixels (49.152 mm x 86.016 mm), which are collected by four divergent cameras. The approximate tilt angles of the sub images are 10˚ in flight direction (x direction) and 20˚ in cross-flight direction (y direction). The pixel size is 12 µm and the focal length is 120 mm. Four low-resolution multi-spectral channels having a pixel size 4 times larger than the panchromatic images are collected using four cameras of size 3k x 2k pixels looking towards nadir. High-resolution multi-spectral images are provided by pansharpening. (Hinz et al. 2000; Tang et al. 2000).

The 12 µm pixel size gives a nominal RP value of 84 lines/mm. In reality the resolution is not constant in the area of the large format virtual image, which is constructed of oblique component images. The image scale decreases with the increasing distance from the image center as shown in Figure 4.

Assuming tilt along one axis only, the size of a pixel in the image border on the ground (x) is obtained from the geometrical relationships (Figure 4). The resolution reduction factor in the border of the component image is 1.5 in the y direction and 1.1 in the x direction. The reduction is larger in the y direction because of the larger tilt angle and the larger image width.

In reality, the sensor is tilted along both the x and y axis, so the relationship is more complicated. The scale reduction factors in the area of one component image in x and y directions are shown in Figure 5. The figure was provided by projecting a regular grid from object to image and comparing the distances of the points to nominal distances calculated by the nominal scale. The factor between the nominal and true scales is

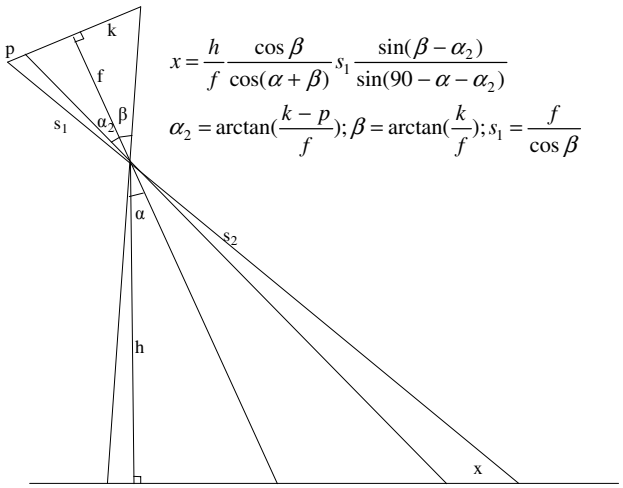

Figure 4. Geometry of a tilted camera. α=tilt angle, h=flying height, p=pixel size in image, f=focal length, k=image side length/2, x=size of image pixel on image border on ground.

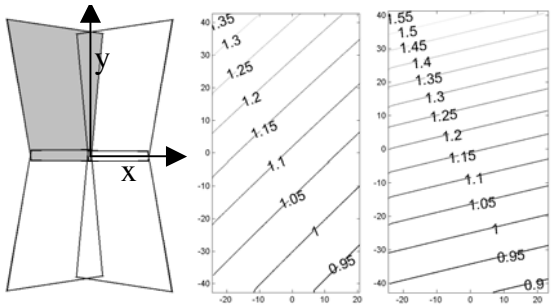

Figure 5. Formation of the large format panchromatic image (left). Resolution reduction factors in x (center) and y-directions (right) for the top-left component image.

between 0.9 and 1.6 in the cross-flight direction and between 0.9 and 1.4 in the flight direction. These reduction factors and the 12 µm pixel size lead to a resolution of between 53 and 84 lines/mm in the cross-flight direction and between 60 and 84 lines/mm in the flight direction.

3.2 MTF

Figure 6 gives the observed MTFs in line pairs per pixel (lp/pixel) of 13 images of block d1_g5 in all, flying, and cross-flight directions. The observed MTFs are given in order not to smooth details; data points are presented in Figure 8. Differences appeared in the MTFs of various images and the behavior was similar with 8 cm GSD. These differences were caused mainly by resolution differences. Some instability appeared especially on the MTFs of sector pairs; the instabilities were mainly caused by the topography of the object. Despite this, the MTFs of DMC appeared to show attractive behavior. The downfall of the MTF at a frequency of 0.4 lp/pixel indicated that the system resolution was lower than the nominal resolution (0.5 lp/pixel).

Figure 7 shows the effect of GSD on the resolution (average all, flight and cross-flight direction MTFs). The MTFs of two blocks with 8 cm GSD were practically the same. The MTF of the 5 cm GSD block was slightly worse than that of the 8 cm GSD blocks.

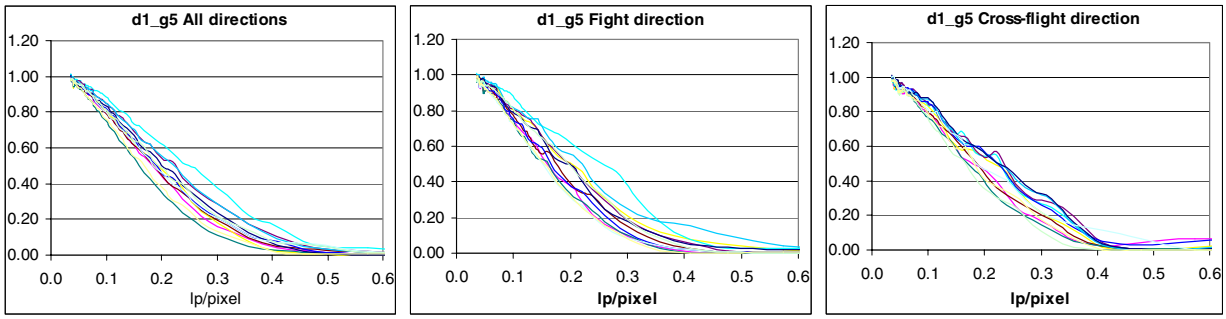

Figure 6. Observed MTFs for 13 images of block d1_g5. Left to right: all, flying, and cross-flight direction.

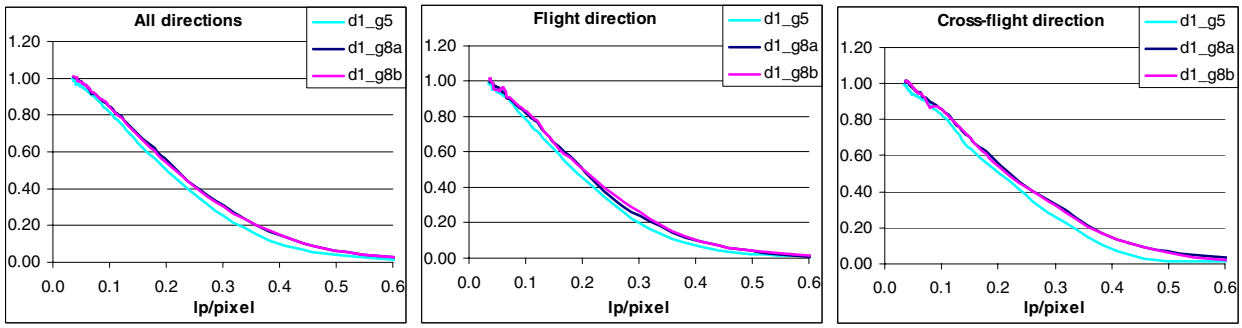

Figure 7. Average MTFs. Evaluation the effect of GSD. Left to right: all, flying, and cross-flight direction.

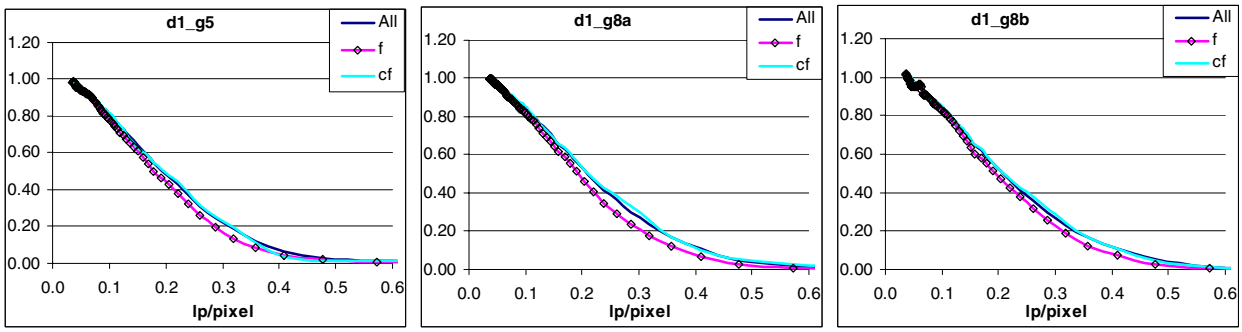

Figure 8. Average MTFs. Evaluation of the effect of flying direction. Left to right: d1_g5, d1_g8a, and d1_g8b.

Figure 8 shows the effect of flight direction on the resolution (average MTFs). In each case the MTF was the best in the cross-flight direction and the worst in the flight direction. In these plots the data points that created the MTFs are also given.

The object modulation was obtained from the Siemens star itself, which is the correct approach only if the GSD is small enough. With too large GSDs, the MTFs become optimistically biased. With an 8 cm GSD, the widest sectors were 12.5 pixels and with a 5 cm GSD the widest sectors were 20 pixels, which should be sufficient. The scale parameter estimated in the MTF calculation should also compensate for this problem.

3.3 Resolving power

The RP values were derived both from the bar targets and from the Siemens star (10% MTF). The RP values in the flight and cross-flight directions are shown for each block as a function of the distance from the image center in Figure 9. Approximate theoretical resolutions are presented for the flight and cross-flight directions (linear functions between minimum and maximum expected RP values; Section 3.1). It appeared that the distance from the image center radically affected the resolution. Central reasons for this behavior are the formation of the large format image from oblique component images and possibly also the decrease of the lens resolution towards the image border. Extensive empirical tests with analog systems have shown similar dependence on the radial distance, but at least partly for different reasons (e.g. Hakkarainen 1986). Comparison to simultaneous analog images indicated quite similar RP values, but the general MTF performance of the DMC was more attractive.

AWAR values are given in Table 2. For instance, the bar targets gave AWAR values of between 61 and 71 lines/mm. AWAR values in the flight direction were 56-68 lines/mm and in the cross-flight direction 65-74 lines/mm. The following average reduction factors from the nominal resolution could be derived:

- GSD 5 cm: flight: 1.5, cross-flight: 1.3
- GSD 8 cm: flight: 1.3, cross-flight: 1.2

On average, the RP values given by the bar targets were 10% higher than the 10% MTF values. The differences between individual images were fairly large, but the average values and general trends were consistent. With 8 cm GSD, the limited size of the bar target caused difficulties for automatic measurement (widest lines were 12 cm).

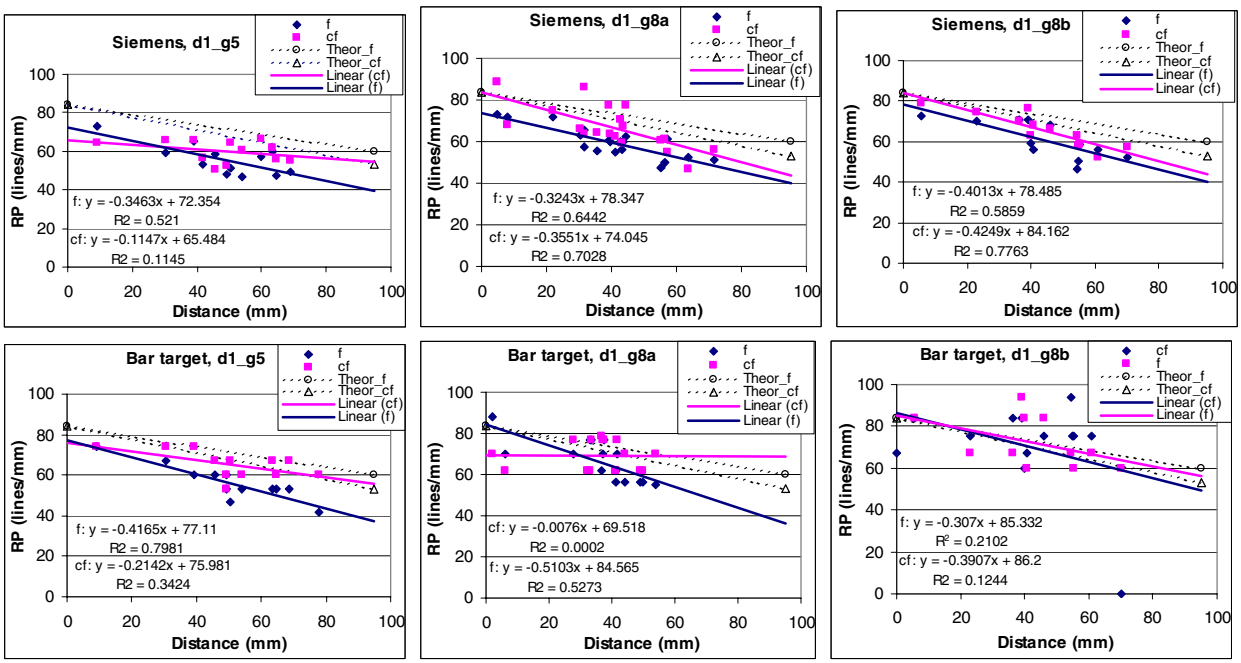

Figure 9. Resolving power measurements as the function of the distance from the image center. Top: 10%MTF from Siemens star, Down: RP from dense bar target. Blocks from left to right: d1_g5, d1_g8a, d1_g8b. (f: resolution in flight direction, cf: resolution in cross-flight direction)

3.4 Resolution of non-pansharpened color images

The MTFs of the non-pansharpened color images were evaluated using the Siemens star. Data from the d1_g5 block was used; the GSD was thus 20 cm. The 10% MTF values are given as a function of the location in Figure 10. The location did not appear to affect the resolution of the color images. The color images had distinctly higher RP-values than the panchromatic images. The green and blue bands had the best resolution (approx. 85 lines/mm) while the red channel had the worst resolution (approx. 80 lines/mm). Resolution of the color images was slightly better in the cross-flight direction than in the flight direction. It is possible that the values were optimistically biased because the 0.2 m GSD is relatively large for the Siemens star used in this study (Section 3.2).

3.5 Image restoration

The images were restored using the methods described by Becker et al. (2005, 2006). Effects of the image restoration on the σ_{PSF} are shown in Figure 11. The restoration resulted in a constant resolution improvement, which was similar for each test block. On average, the σ_{PSF} values of the restored images were better than those of the original images by a factor of 1.4.

Table 2. Average resolution (direction f: flight, cf: cross-flight).

		d1_g5	d1_g8a	d1_g8b
AWAR	Siemens	58	59	61
(lines/mm)	Bar	61	64	71
AWAR_f	Siemens	56	56	58
(lines/mm)	Bar	56	59	68
AWAR_cf	Siemens	60	63	63
(lines/mm)	Bar	65	69	74
Average σ_{PSF}	All	0.48	0.44	0.45
(pixel)	Flight	0.52	0.49	0.48
	Cross-flight	0.48	0.44	0.44

4. SUMMARY AND CONCLUSIONS

The resolution of an Intergraph DMC large-format photogrammetric camera was studied using extensive empirical test flight data. The parameters of the study were the flight direction, the flying height and the distance from the image center.

The analysis showed that the resolution of the large-format panchromatic images was dependent on the distance from the image center. One important reason for this behavior is that the component images are oblique, which causes smaller scale and reduces the resolution towards the image border. Also the reduction of the lens resolution towards the image borders can contribute to the phenomenon. Details of the lens MTFs would make more detailed analysis of the effect of various factors possible. The resolution of the vertical non-pansharpened color images was not affected by distance from the image center.

Evaluation of the effect of the flying direction showed that the resolution was worse in the flight direction than in the cross-flight direction. One possible reason for this could be a slight insufficiency of the forward motion compensation. The resolution appeared to improve with increasing GSD. The probable reason for this is that the image motion is relatively smaller when the GSD is larger. It is possible that these phenomena are related to the entire imaging system. The test flights were performed using a low flying altitude with relatively high flying speed; different conditions might lead to different results.

In the future, field calibration will be used increasingly to test and validate photogrammetric systems. It is important to include resolution evaluation in the field calibration process. In this study, MTF, point spread function, and resolving power were used as measures of quality. High efficiency and objectivity were achieved by automated measurement methods.

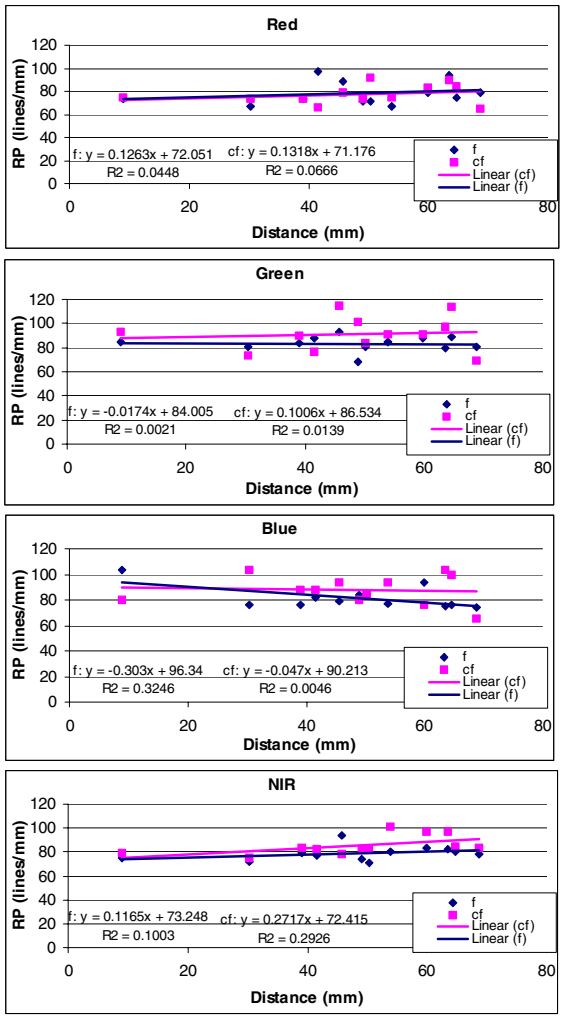

Figure 10. RP (10%MTF) of the color channels.

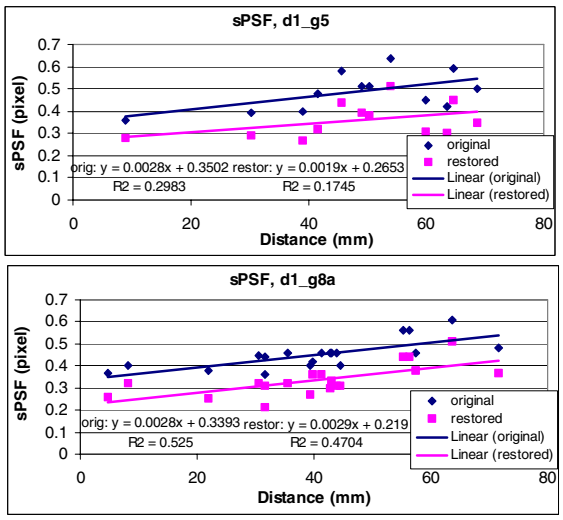

Figure 11. Effect of image restoration on σ_{PSF}.

AUTHOR CONTRIBUTIONS

E. Honkavaara designed the empirical tests, supervised the development of the methods at the FGI, performed most of the analysis and compiled the text. J. Jaakkola is the author of the RESOL software (Section 2.2), and he performed all the empirical measurements at the FGI and participated in the data analysis. L. Markelin took care of the processing of the DMC images and helped to develop the MTF method (Section 2.2.2). S. Becker gave the details of the Stuttgart method for MTF determination, which formed the basis of the MTF method (Section 2.2.2), and performed the empirical study in Section 3.5.

ACKNOWLEDGEMENTS

The test flights were performed in co-operation with the National Land Survey of Finland (NLS), whose support and valuable comments are greatly appreciated. Particularly the assistance given by several individuals at the FGI is appreciated. Intergraph is acknowledged for their comments concerning the results and for providing information on technical details of the DMC.

REFERENCES

Ahokas E., Kuittinen R., Jaakkola J, 2000. A system to control the spatial quality of analog and digital aerial images. International Archives of Photogrammetry and Remote Sensing, Vol. 33. Pp. 45-52.

Becker, S., Haala, N. , Reulke, R., 2005. Determination and Improvement of Spatial Resolution for Digital Aerial Images. In proceedings of ISPRS Hannover Workshop High-Resolution Earth Imaging for Geospatial Information. On CD.

Becker, S., Haala, N., Honkavaara, E., Markelin, L., 2006. Image restoration for resolution improvement of digital aerial images: A comparison of large format digital cameras. This proceedings.

Coltman, J. W., 1954. The specification of image properties by response to sine wave input, Journal of the Optical Society of America, Vol. 44, No. 6, pp. 468-471.

Hakkarainen, J., 1986. Resolving power of aerial photographs. Surveying Science in Finland, 1986, no. 2, pp. 8-59.

Hinz, A., Dörstel, C., Heier, H., 2000. Digital Modular Camera: System Concept and Data Processing Workflow. International Archives of Photogrammetry and Remote Sensing, Vol 33, Part B2, pp.164-171.

Honkavaara, E., Jaakkola, J., Markelin, L., Peltoniemi, J., Ahokas, E., Becker, S., 2006. Complete photogrammetric system calibration and evaluation in the Sjökulla test field – case study with DMC, Proceedings of EuroSDR Commission I and ISPRS Working Group 1/3 Workshop EuroCOW 2006, CD-ROM, 6 pages.

Kuittinen R., Ahokas E., Högholen A., Laaksonen J, 1994. Test-field for Aerial Photography. The Photogrammetric Journal of Finland. Vol. 14, No 1, pp. 53-62.

Kuittinen, R,. Ahokas, E., Järvelin, P., 1996. Transportable test-bar targets and microdensitometer measurements – a method to control the quality of aerial imagery. International Archives of Photogrammetry and Remote Sensing, Vol. 31, Part B1, pp. 99-104.

Read, R.E, Graham, R.W., (2002). Manual of Air Survey: Primary Data Acquisition. Whittles Publishing, Caithness, 408 p.